



A novel approach toward the bio-inspired synthesis of CuO nanoparticles for phenol degradation and antimicrobial applications

Harshal Dabhane¹ · Suresh Ghotekar² · Manohar Zate³ · Kun-Yi Andrew Lin⁴ · Abbas Rahdar⁵ · Balasubramani Ravindran^{6,7} · Dhanraj Bahiram¹ · Chetan Ingale⁸ · Bhushan Khairnar⁹ · Deepali Sali¹⁰ · Sagar Kute¹¹ · Ghanshyam Jadhav¹² · Vijay Medhane^{12,13}

Received: 10 November 2022 / Revised: 10 February 2023 / Accepted: 14 February 2023
© The Author(s), under exclusive licence to Springer-Verlag GmbH Germany, part of Springer Nature 2023

Abstract

Nanotechnology has been a widespread field for the last decade, but the clean and sustainable development of nanomaterials is a stimulating task for researchers in the current situation. The green synthesis of nanomaterial using plant extract is the most practiced chore of researchers, but the use of inorganic and organic bases makes them valueless. Herein, we first report the biogenic synthesis of copper oxide nanoparticles (CuO NPs) using human urine as a reducing agent. The XRD analysis confirmed the crystalline nature and synthesis of CuO NPs, where the grain size was found to be 6.78 nm. The absorption-desorption study of human urine-mediated synthesized CuO NPs was done with the BET technique, and the pore volume and surface area were found to be 0.06 cm³/g and 92.64 nm, respectively. Finally, the spherical morphology was confirmed by SEM analysis, and elemental analysis confirmed the formation of CuO NPs using human urine. The well-characterized CuO NPs were used for the eco-friendly degradation of phenol in aqueous media under sunlight, and the removal efficiency was recorded using a spectrophotometer. The antibacterial activity of synthesized CuO NPs was tested against gram-positive and gram-negative pathogenic bacteria. Also, the antifungal activity was verified against different fungal strains.

Keywords Bio-inspired synthesis · CuO NPs · Human urine · Photocatalytic activity · Antimicrobial activity

Abbreviations

BET	Brunauer-Emmett-Teller
BJH	Barrett-Joyner-Halenda
EDX	Energy-dispersive X-ray spectroscopy
FTIR	Fourier-transform infrared spectroscopy
CuO NPs	Copper oxide nanoparticles
MIC	Minimal inhibitory concentration
mm	Millimeter
NPs	Nanoparticles
PL	Photoluminescence
SEM	Scanning electron microscopy
TEM	Transmission electron microscopy
UVDRS	Ultraviolet visible diffuse reflectance spectroscopy
XRD	X-ray diffraction

1 Introduction

Nanotechnology is the most widely studied research subject, owing to its numerous multifunctional applications in diverse fields [1–3]. As a result, modern nanotechnology significantly contributes to energy, healthcare products, nanomedicine, defense, bioremediation, and catalysis [4–11]. Numerous researchers have reported various techniques over time, but the report gains value if the method follows the principles of green chemistry [12–14]. Physical, chemical, and biological approaches are employed to synthesize multifunctional nanomaterials in a top-down and bottom-up approach [15–18]. The main concern is whether the stated approach is environmentally benign or not. To address this, the researchers used a biological process that avoids using toxic chemicals and high energy [19–21]. Therefore, the biological method is successful in grabbing the attention of researchers due to its features like being eco-friendly, quick, safe, and economical, and not consuming more energy [22, 23].

The environment and aquatic life are two of the most basic needs of all living beings on the planet, and the entire globe is working on projects to protect the environment

✉ Suresh Ghotekar
ghotekarsuresh7@gmail.com

Extended author information available on the last page of the article

and keep it safe and alive through various means [24]. However, as humanity evolves through industrialization and civilization, they wreak havoc on the environment [25]. As a result, human society is currently attempting to reduce pollution caused by industrialization [26]. Different industries deposit their waste and byproducts into water bodies [27, 28], endangering aquatic and human life [29–31]. For example, phenol is a common byproduct of dyes, paints, pharmaceuticals, agrochemicals, and other industries [31]. The World Health Organization has set the permissible limit of phenol in drinking water at 1 g/L [32]. There are diverse ways to remove or degrade phenol from water sources, including flow injection, liquid chromatography, the Gibbs method, fluorescence, and chemical sensors. However, these methods have yet to be proven effective [33]. Countable publications have been published in the last decade on the degradation of phenol using synthesized nanoparticles (NPs). This technology is appealing since it is quick, inexpensive, and safe and can be used for large amounts of water purification [4]. A literature survey reveals the synthesis of CuO NPs using reflux and precipitation methods for the degradation of phenol [31]. However, the other nanomaterial, also synthesized via different methods [34], was reported as a photocatalyst in the presence of sunlight and UV light [35–39].

The CuO NPs are p-type semiconductors having an average band gap of 1.2 eV. That is why they are effectively used as sensors, electronic devices, solar energy transformation, battery semiconductors, and field emissions [40–42]. Due to the fascinating applications of CuO NPs, far more research has been done on them. CuO NPs have recently grabbed the attention of researchers due to their effective catalytic and biological activity [43–47]. CuO NPs also have the finest photocatalytic activity, and numerous researchers have reported organic pollutant degradation utilizing CuO NPs synthesized using various methods [48–51]. Plant extract is the most useful method for synthesizing NPs in the current scenario. Nevertheless, in the case of plant extract-mediated synthesis of NPs, the basic condition must be maintained by adding an organic or inorganic base (NH_3 , NaOH , etc.) [52, 53]. Our goal is to synthesize CuO NPs without adding an external base.

Furthermore, CuO NPs are applied in catalysts, superconductors, batteries, gas sensors, and other devices. For this reason, CuO NPs are remarkably effective in antimicrobial and anticancer treatments. Regularly occurring CuO NPs have been found in pharmaceutical, cosmetic, and semiconductor applications [40]. They can also be found in most ointments, where they act as antimicrobial agents against disease-affected cells. Compared to other types of NPs, CuO NPs are safe and have low toxicity toward living cells [54]. As a result, they can be used to treat serious illnesses brought on by fungi, common bacteria, intestinal

bacteria, and urine bacteria in the body [55]. Small CuO NPs made from plant material has a high potential for effectiveness in anticancer, antioxidant, and antimicrobial applications due to their ability to interact adhesively with bacterial or fungal cell surface through Van der Waals forces and electrostatic forces [41].

Herein, the present study report, for the first time, bio-inspired synthesis of CuO NPs using human urine and copper acetate as a precursor. In this study, we mainly focus on the one-step biogenic synthesis of CuO NPs using human urine, which is economical, quick, safe, and eco-friendly, and its mechanism of formation. Spectroscopic and microscopic methods confirmed the synthesis of CuO NPs. Next, we have evaluated the benefits of biogenic synthesized CuO NPs for antimicrobial and catalytic activities.

2 Material and methods

2.1 Material

The morning urine of humans (male) was collected in a 1-L plastic clean and dry bottle. The analytical grade copper acetate was purchased from Sigma-Aldrich, India, and used without further purification.

2.2 Optimization of synthesis of CuO NPs using human urine

The colorimetric experiment was used to optimize the synthesis of CuO NPs. Briefly, 1 mL of human urine was put into five clean test tubes labeled 1 to 5. After adding the 1 M copper acetate solution to each test tube in various proportions ranging from 1 to 5 mL, all test tubes were placed in a sonicator for 5 min. The resulting product was allowed to settle before being filtered through a Buchner funnel, and the filtrate was then used for colorimetric analysis. At 635 nm, the absorbance of the filtrate (unreacted copper acetate) was measured. The lowest absorbance was observed for 1 mL of human urine and 1 mL of 1 M copper acetate solution (Fig. 1). As a result, the lowest amount of human urine required to precipitate is 1 mL of 1 M copper acetate solution. Based on this optimization result, the preparation of CuO NPs was done.

2.3 Bio-inspired synthesis of CuONPs

Human urine was selected as the surfactant to begin a novel synthesis of CuO NPs. The morning urine of a healthy person was collected in a dry and clean bottle and filtered through Whatman filter paper no. 41 to remove the unwanted impurities and further use for preparing CuO NPs.



Fig. 1 Optimization for the synthesis of CuO NPs using human urine

A 100-mL copper acetate solution having a concentration of 1M was prepared by dissolving 1.82g copper acetate in 100 mL of double-distilled water in a volumetric flask and dropwise adding 100 mL of human urine taken in a 250-mL beaker via dropping funnel at room temperature. After successfully adding copper acetate solution to human urine with constant stirring, a green color precipitate was obtained. Once the precipitation was completed, it was allowed to settle down and washed three times with double-distilled water to remove the unreacted matter. Finally, the precipitate was filtered through a Buchner funnel and dried at 100 °C in an air oven. The dried precipitate was further calcinated in a muffle furnace at 400 °C for 2 h, resulting in brown-black-colored CuO NPs.

2.4 Characterization

The synthesis of CuO NPs using human urine was confirmed by a UV-DRS spectrometer (JASCO V-770), and the band gap was obtained by plotting $(\alpha h\nu)^2$ against $h\nu$ according to the Tauc equation. The bond formation and strength in Cu and O atoms were studied by FT-IR spectroscopy (FT/IR-4600type A). The photoluminescence activity was also evaluated using the photoluminescence spectrum (FP-8200). The surface area and porosity of synthesized CuO NPs were evaluated by an adsorption-desorption study (BET). In contrast, XRD, SEM (VEGA3 TESCAN), and EDX techniques confirmed the morphology and elemental composition. Additionally, TEM (PHILIPS CM200) was utilized further to affirm the particle size and topology of CuO NPs.

2.5 Photocatalytic activity of synthesized CuONPs

The photocatalytic efficiency of human urine-mediated CuO NPs was investigated by offering phenol degradation under sunlight. In the present experiment, 50 mL of aqueous solution (500 ppm) of phenol was taken in a 100-mL beaker with 15 mg of synthesized catalyst CuO NPs stirred on a magnetic stirrer in the presence of sunlight. The progress of the reaction was examined by recording the absorbance of the reaction mixture using a UV-visible spectrophotometer at wavelength 279 nm.

Equation (1) was used to compute the degradation efficiency,

$$\text{Efficiency (\%)} = (C_0 - C_t) / C_0 \times 100 \quad (1)$$

C_0 is the initial absorbance at $t = 0$, and C_t is the absorbance value at a particular time interval.

2.6 Antimicrobial study of synthesized CuO NPs

A literature survey supports the antimicrobial efficiency of CuO NPs. Hence, human urine-mediated CuONPs were tested against different bacterial strains (*Staphylococcus aureus*, *Bacillus subtilis*, *E. coli*, and *P. mirabilis*) and fungal strains (*Candida albicans* and *Aspergillus niger*) using the disc diffusion method [56], and the obtained result was compared with the standard streptomycin for bacteria and fluconazole for fungus.

3 Result and discussion

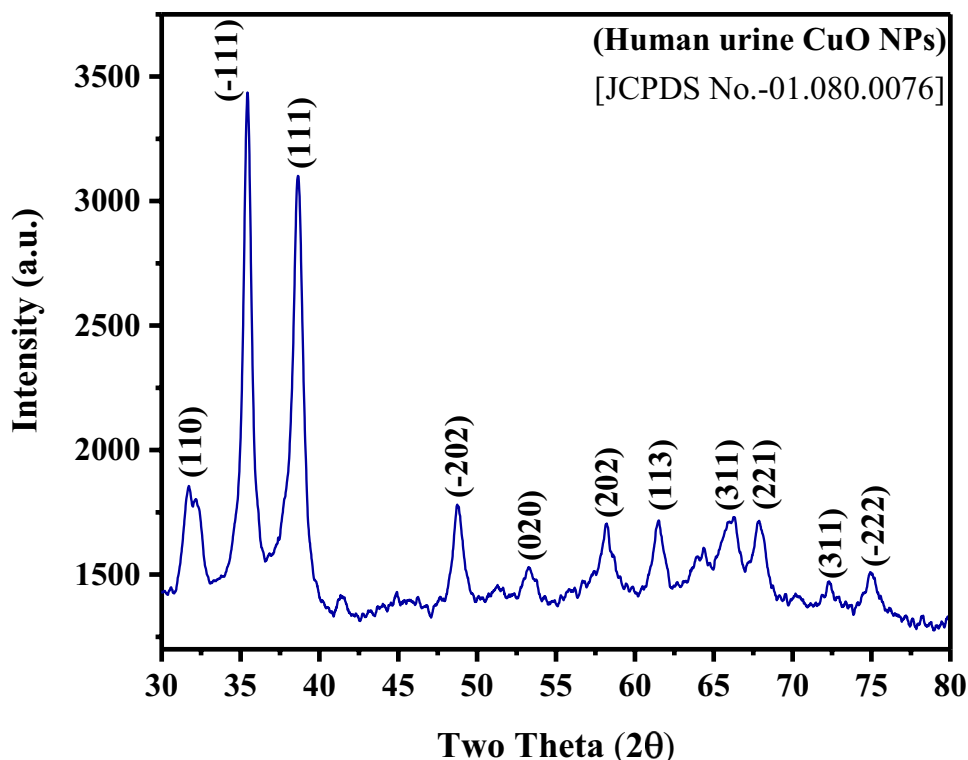
3.1 X-ray diffraction analysis

The X-ray diffraction technique helps to find out the crystal structure and size of synthesized NPs, and the XRD spectrum of human urine-mediated synthesized as shown in Fig. 2. The clear peaks at 2θ are 31.72°, 35.40°, 37.89°, 48.88°, 53.34°, 58.10°, 61.49°, 66.34°, 67.99°, 72.45°, and 74.88° assigned as (110), (−111), (111), (−202), (020), (202), (113), (311), (221), (311), and (−222) respectively. All peaks are highly consistent with the JCPDS card No. 01.080.0076 of CuO NPs of the monoclinic phase [57]. The grain size of synthesized CuO NPs was calculated using Scherrer's formula (2).

$$D = K\lambda / \beta \cos\theta \quad (2)$$

where K is constant (0.9), λ is the wavelength of X-ray (1.54056 Å), β is the corrected full width of half maximum, and θ is Bragg's angle [14]. The peak obtained in the XRD spectrum of human urine-synthesized CuO NPs was evaluated with the help of the origin software. The average size

Fig. 2 XRD pattern of human urine-mediated CuO NPs



of synthesized CuO NPs was calculated using Scherrer's equation, which was found to be 6.77 nm.

3.2 Morphological and elemental analysis

The SEM technique investigated the morphology of human urine-mediated CuO NP synthesis. The SEM micrograph of synthesized CuO NPs is seen in Fig. 3. SEM validates the spherical morphology with unequal size. At the same time, the purity and elemental composition of CuO NPs were determined using the EDS technique, as shown in Fig. 4. Four distinct peaks were observed in the EDS graph, including at 0.5 KeV, 1 KeV, 8 KeV, and 9 KeV, demonstrating the purity and production of CuO NPs from human urine.

Additionally, the TEM study has been conducted to examine the topology and particle size of CuO NPs further. According to the findings, CuO NPs had a pseudo-spherical shape due to the agglomeration and ranged in size from 5 to 60 nm, as shown in Fig. 5. The TEM result magnifies and clearly shows that the produced CuO had a nanoscale scale, which was previously determined through characterization using XRD profile.

3.3 Optical properties

The optical study of nanoparticles depends on the surface properties, where the absorption maxima are affected by

the size and morphology of nanoparticles. The UV-DRS analysis of human urine-mediated CuO NPs shows a single intense peak at 296.76 nm, shown in Fig. 6, which confirms the formation of CuO NPs and is supported by the previous report [57]. The optical band gap of human urine-fabricated CuONPs was calculated using Tauc's Eq. (3),

$$\alpha h\nu = (h\nu - E_g)^n \quad (3)$$

where α is the absorption coefficient, $h\nu$ is the photon energy, while E_g represents the optical band gap of synthesized CuO NPs. The optical band gap of human urine-mediated CuONPs was found to be ($E_g = 3.29$ eV), shown in the inset of Fig. 6, and observed like a blue shift when compared with the previous report ($E_g = 3.11$ eV) [58]. The photoluminescence spectrum of synthesized nanoparticles is a function of their size and morphology, as seen in the photoluminescence spectra of human urine-fabricated CuO NPs (Fig. 7). The spectrum exhibits a single orange emission peak located at 596.83 nm.

3.4 Adsorption-desorption study

The surface analysis of the human urine-mediated synthesis of CuO NPs was done with the help of Brunauer-Emmett-Teller (BET) analysis of a nitrogen atmosphere. The surface properties of synthesized CuO NPs, like specific surface area, pore size, and volume distribution, are shown in Fig. 8. The surface area of CuO NPs was found to be $3.05 \text{ m}^2/\text{g}$,

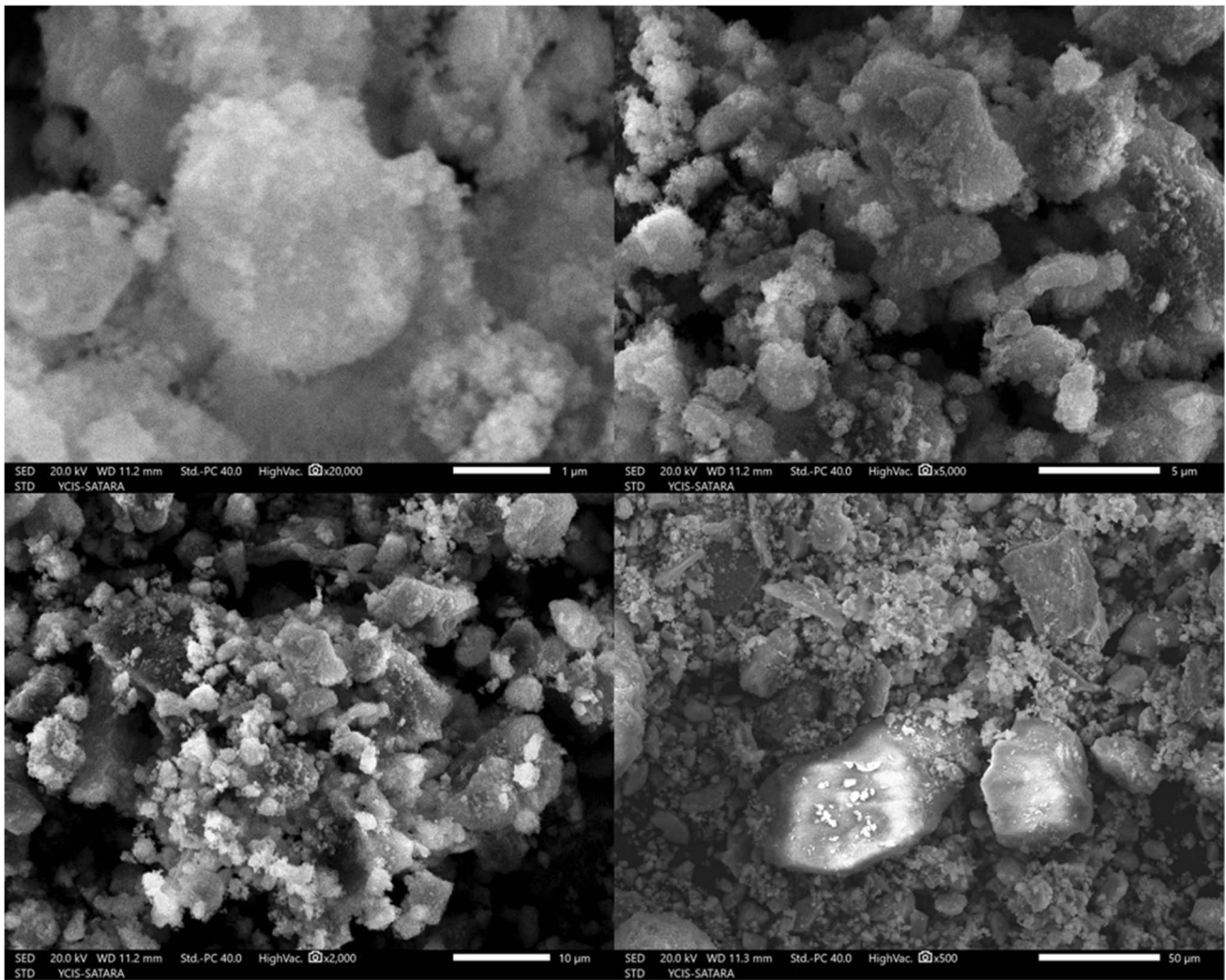


Fig. 3 SEM pictogram of the human urine-mediated CuO NPs

Fig. 4 EDX spectrum of the human urine-mediated CuO NPs

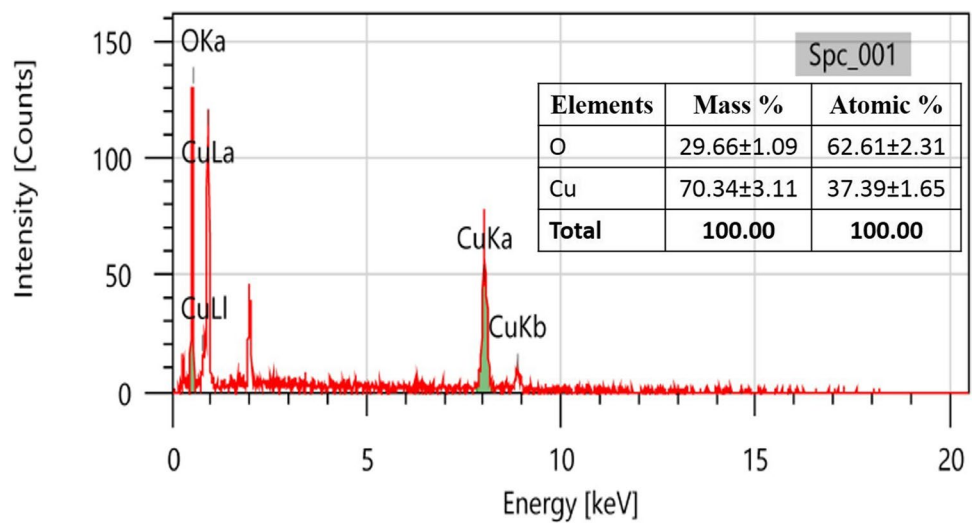


Fig. 5 TEM images of human urine-mediated CuO NPs

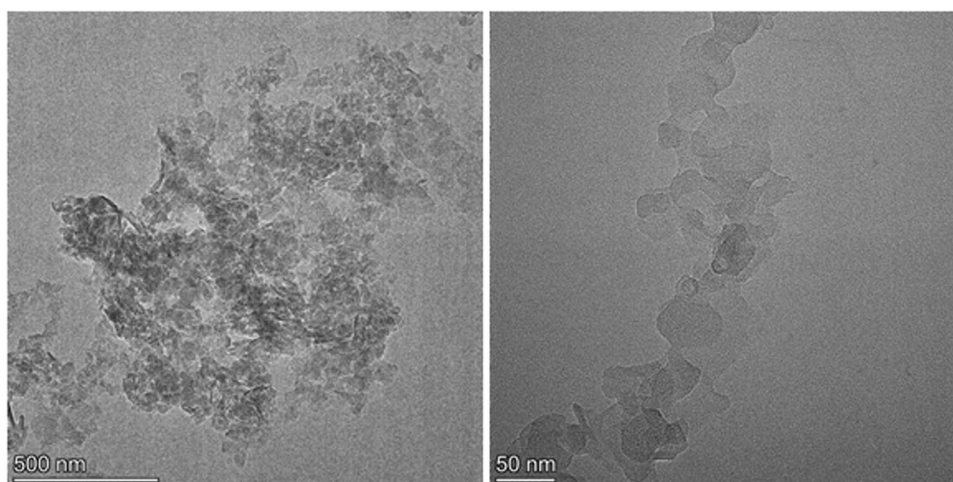
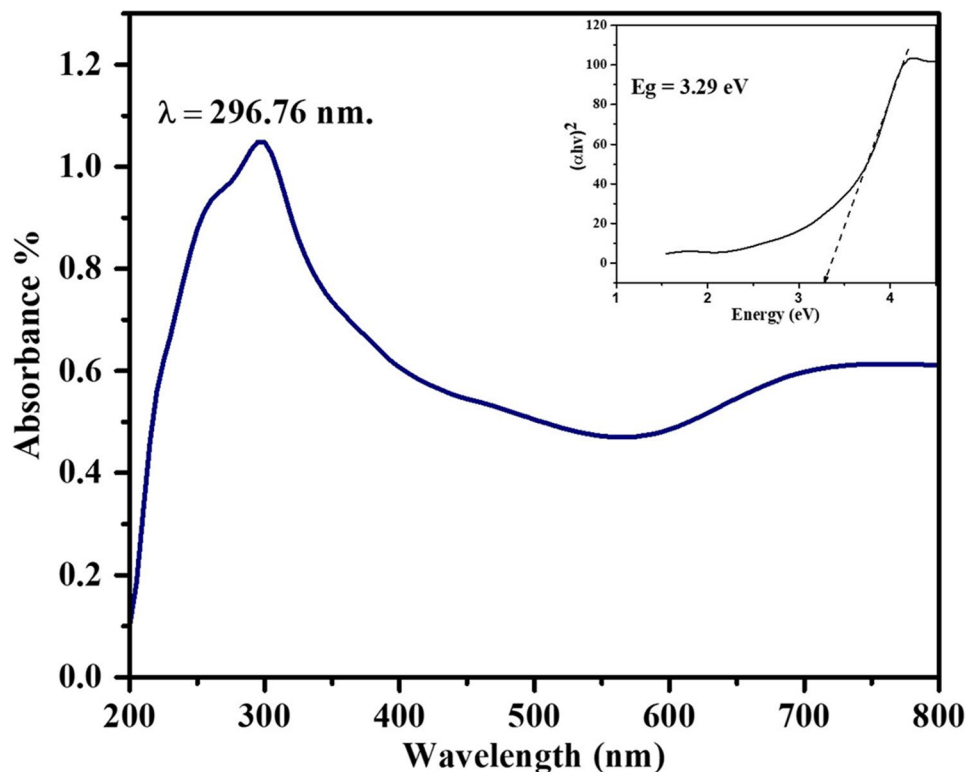


Fig. 6 UV-DRS spectrum and band gap of human urine-mediated CuO NPs



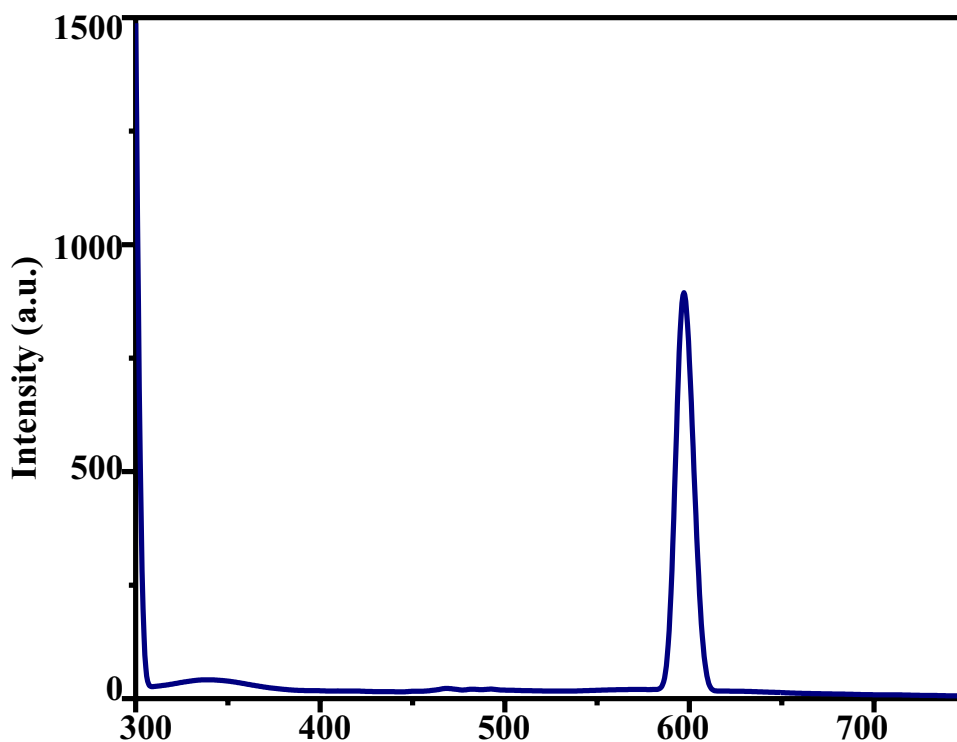
whereas the average size and pore volume, were found to be 92.64 and 0.062 cm³/g, respectively [59].

3.5 FT-IR analysis

The FTIR spectra of the human urine and fabricated CuO NPs are displayed in Fig. 9a and b. In Fig. 9a, the broad peak that occurred at 3340 cm⁻¹ is due to the stretching frequency of -OH, and the peak at 1635 cm⁻¹ is associated with an N-H bond and is assigned to the biomolecules

(urea, creatinine, and uric acid) present in the fuel (reducing agent). A metal-oxygen bond was examined using the FT-IR spectrum of CuO NPs (Fig. 9b). The functional group region was used to confirm the involvement and presence of biomolecules in the nanomaterial synthesis. The two significant peaks at 624 cm⁻¹ and 560 cm⁻¹ confirm the formation of the Cu-O bond in the FT-IR spectrum of human urine-mediated CuO NP synthesis (Fig. 9b). The peaks at different energies of 3448 cm⁻¹ and 3341 cm⁻¹ may be attributable to amine (-NH) and hydroxyl (-OH) group

Fig. 7 Photoluminescence spectrum of human urine-mediated CuO NPs



stretching. Finally, 1057 cm^{-1} confirms the presence of alkene and C–O functional groups, respectively [60]. However, the weak band may be due to the absorption of atmospheric moisture by KBr during the pelletization of the CuO NPs, as KBr is more hygroscopic [61].

3.6 A plausible mechanism for bio-inspired synthesis of CuO NPs

Figure 10 depicts the biomolecules (Fig. 11) found in human urine [62] to explain how the copper acetate can alter into CuO NPs. The proposed reaction mechanism demonstrates how active bio-molecules behave as stabilizing and reducing agents. However, urea has been selected as a sample molecule to suggest the mechanism. Because the polar sides of urea adhere to copper ions; copper and urea form a stable complex and result in the precipitate in the form of copper

hydroxide in the basic condition of human urine. After calcination, the complex decomposes and forms CuO NPs.

3.7 Photocatalytic activity

The photocatalytic property of a material is defined by its semiconducting nature; the UV-DRS spectra of human urine-mediated synthesized CuO NPs confirm the 3.29-eV band gap, indicating that it is capable of photocatalytic phenol degradation. In this experiment, a 500-ppm phenol solution was prepared in water as a solvent and left in the dark for 2 h to achieve the adsorption-desorption equilibrium. After that, two sets of 50 mL of aqueous phenol solution in a 100-mL beaker with 30 mg CuO NPs were made, one set was maintained in the dark, and the other set was used for further investigation. Finally, the phenol solution containing the catalyst was stirred in sunlight on a magnetic

Fig. 8 **a** Adsorption-desorption study, **b** surface parameters of the human urine-mediated CuO NPs

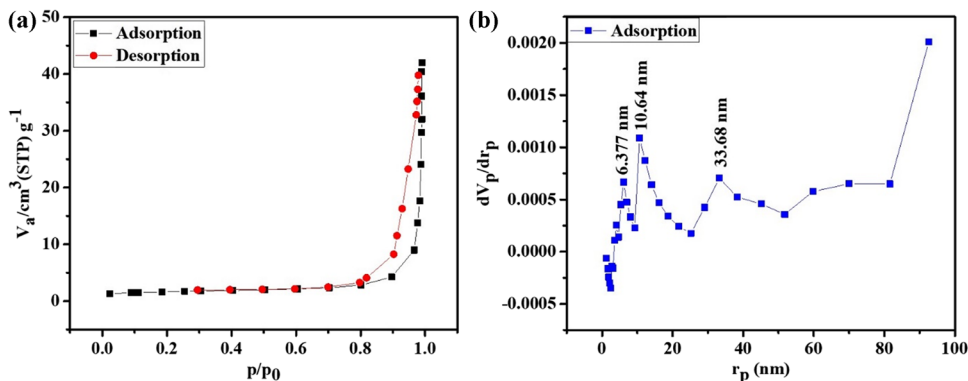
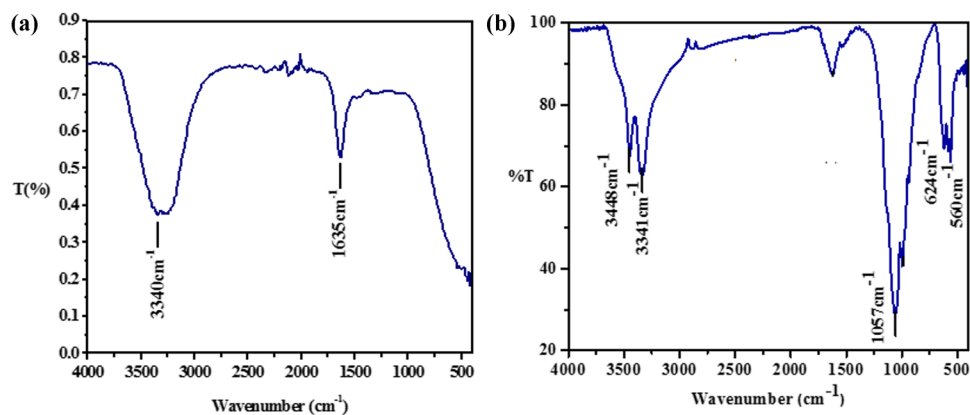


Fig. 9 FT-IR spectra of **a** human urine and **b** synthesized CuO NPs



stirrer, and absorbance was measured using a double-beam spectrophotometer at a regular time interval of 15 min at a wavelength of 279 nm. Figure 12a depicts a steady decrease in absorbance over time; Fig. 12b explains the percent removal effectiveness of produced CuO NPs in phenol solution; and Fig. 12c confirms the reaction's first-order mechanism. The current work was compared to earlier publications and discovered that human urine-mediated produced CuO NPs degraded 50 mL 500 ppm phenol solution with 30 mg catalyst in just 215 min under sunlight. By graphing percent degradation efficiency against time intervals, the percent removal efficiency was estimated to be 79.41% in 215 min.

The band gap and surface area also determined the photocatalytic efficiency of the synthesized material. The high surface area of CuO NPs is confirmed by the N_2 adsorption-desorption analysis, which supports the strong catalytic activity of CuO NPs in the degradation of phenol. In addition, a putative mechanism for photocatalytic phenol degradation was demonstrated (Fig. 13). The synthesized CuO NPs behaved as semiconductors in the presence of sunlight, absorbing the solar radiation, resulting in the excitation of electrons from the valance band (VB) to the conduction band (CB), the formation of holes, and free electrons at VB and CB, which were responsible for the subsequent reaction. The holes and free electrons react with water and oxygen molecules and generate radicals. These radicals combine with phenol and are converted into intermediates and further degrade into eco-friendly molecules like CO_2 and water, as shown in (Fig. 13).

In most cases, the photocatalyst was made using non-eco-friendly physical and chemical methods, most of which were activated using UV light. Compared to the earlier work [31], the CuO NPs were synthesized using a novel, environmentally friendly method involving human urine. The photocatalytic degradation of phenol was carried out in the presence of solar light rather than UV light. The maximum phenol concentration (500 ppm) was degraded in 215 min with 79.41% efficiency. As a result, human urine-mediated synthesized CuO NPs are one of the most efficient and environmentally benign photocatalysts available. However,

according to the literature, phenol degradation using biosynthesized CuO NPs has yet to be reported.

3.8 Antimicrobial efficacy

In the present study, the antibacterial activity of human urine-mediated synthesized CuO NPs tested against gram-positive and gram-negative bacterial strains is shown in Fig. 14. The zone of inhibition exhibited by synthesized CuO NPs at the same concentration of 1 mg/mL with reproducibility against the bacterial pathogens (*S. aureus*, *B. subtilis*, *E. coli*, *P. mirabilis*) is given in Table 1. Streptomycin is used as a control. The antibacterial activity of synthesized CuO NPs was graphically compared with the standard streptomycin drug with error bars and shown to be well in Fig. 15. The MIC study was also done with the same bacterial strain, and the result is shown in Table 1.

Furthermore, the synthesized CuO NPs also screen for antifungal activity against two fungal strains (*C. albicans* and *A. niger*) shown in Fig. 16. The zone of inhibition of human urine synthesized CuONPs and MIC study is shown in Table 2, where fluconazole was taken as a control. The activity was shown by synthesized CuO NPs graphically compared with standard and found to be effectively shown in Fig. 17. When compared to plant extract-mediated CuO NPs, human urine-derived CuO NPs had excellent antifungal efficacy [63–65].

The proposed mechanism of antibacterial activity of human urine-mediated synthesized CuO NPs is shown in Fig. 13. The free radical generated after the excitation of electrons from VB to CB due to the absorption of solar energy reacts with the bacterial cell wall and inhibits the growth of the bacterial strain.

The microbial system's inhibition mechanism has been explained in several directions.

- i. The CuO NPs dispersed and expanded on the surface of microbes due to the attraction of electrostatic charges present amidst them.

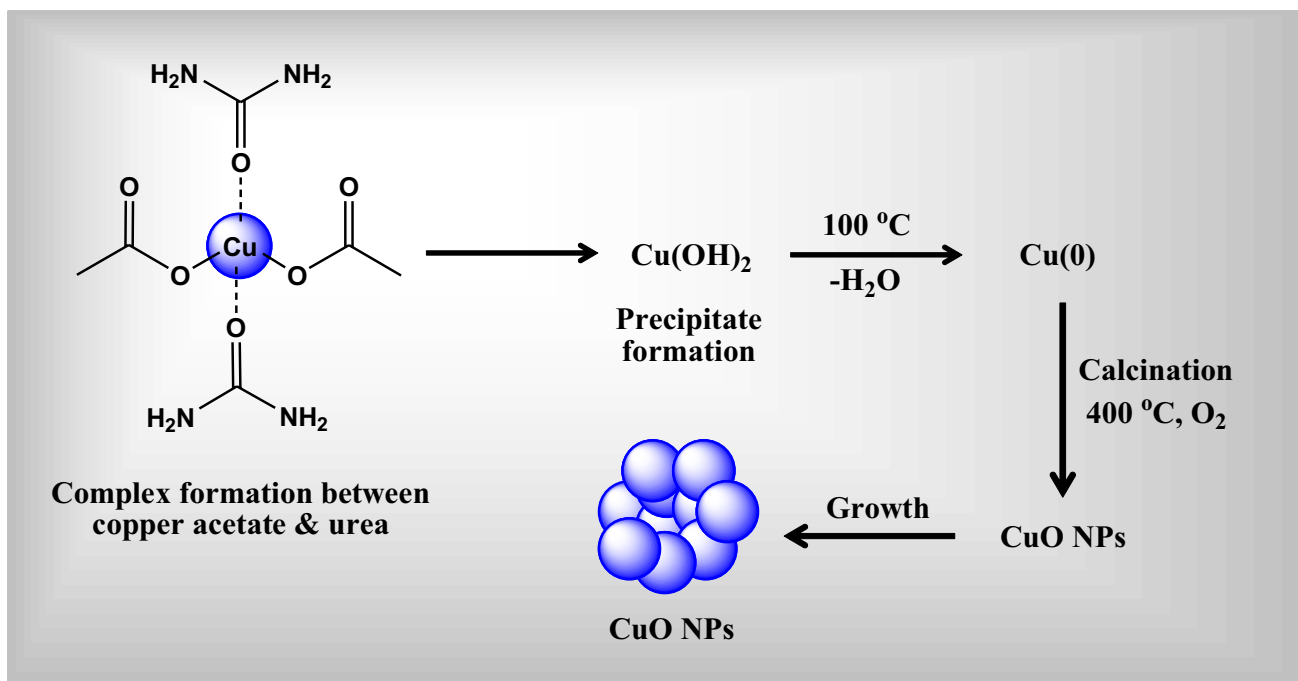
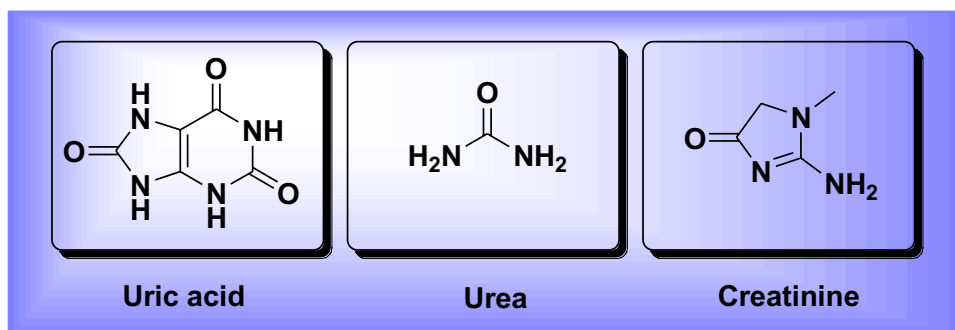


Fig. 10 Active biomolecules in human urine

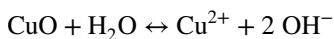
Fig. 11 A proposed mechanism for the synthesis of CuO NPs using human urine



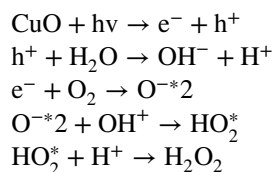
- ii. The adhered CuO NPs disrupted the cell wall. It causes stretching of the cell membrane and accelerates cell damage and death.
- iii. The Cu²⁺ ions are freely liberated from CuO NPs. The DNA is damaged by reactive oxygen species such as hydrogen peroxide (H₂O₂), OH⁻ radicals, and O₂⁻² ions, preventing cell proliferation.

CuO NPs contained positively charged ions bonded to the negatively charged microbial surface, harming the cell [66]. The large surface area of the CuO in the nanoscale increases the toxicity of Cu atoms on microbial cells.

The Cu⁺ ions liberating mechanism was,

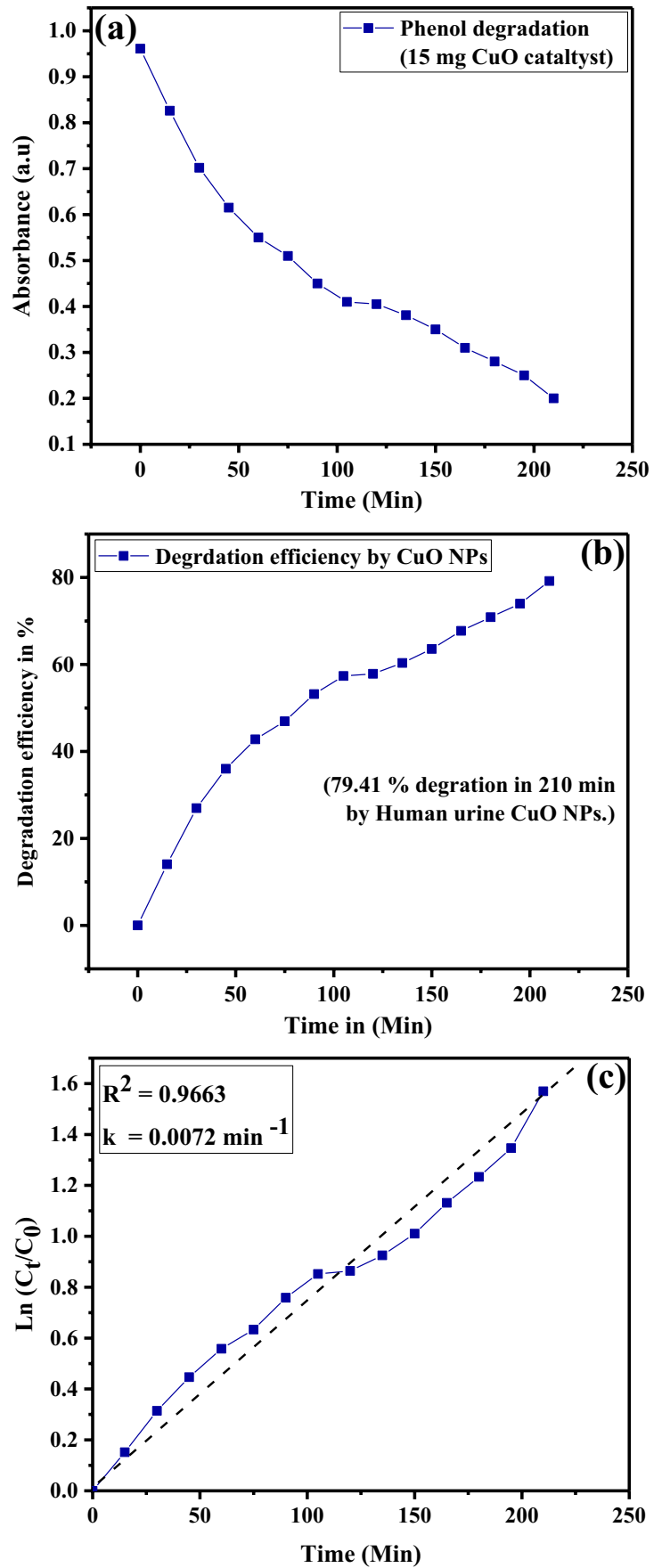


The reaction mechanism was,



The released Cu²⁺ ions damage all the applied microorganisms' cell walls. These ions harm the cell wall. This process served as the impetus for the bacterial cell's internal cytoplasmic contents to be released. Small-sized CuO NPs released Cu²⁺ ions from their place of attachment. The adhesive nature of their contact with the bacterial cell surface produced by Van der Waals and electrostatic forces favored cell damage [66, 67]. These findings have been compared to earlier reports (Table 3).

Fig. 12 Photocatalytic activity of human urine-mediated CuO NPs; **a** plot of absorbance vs. time in minutes for the degradation of phenol under sunlight, **b** degradation efficiency (%) of phenol by CuO NPs, and **c** its first-order kinetics



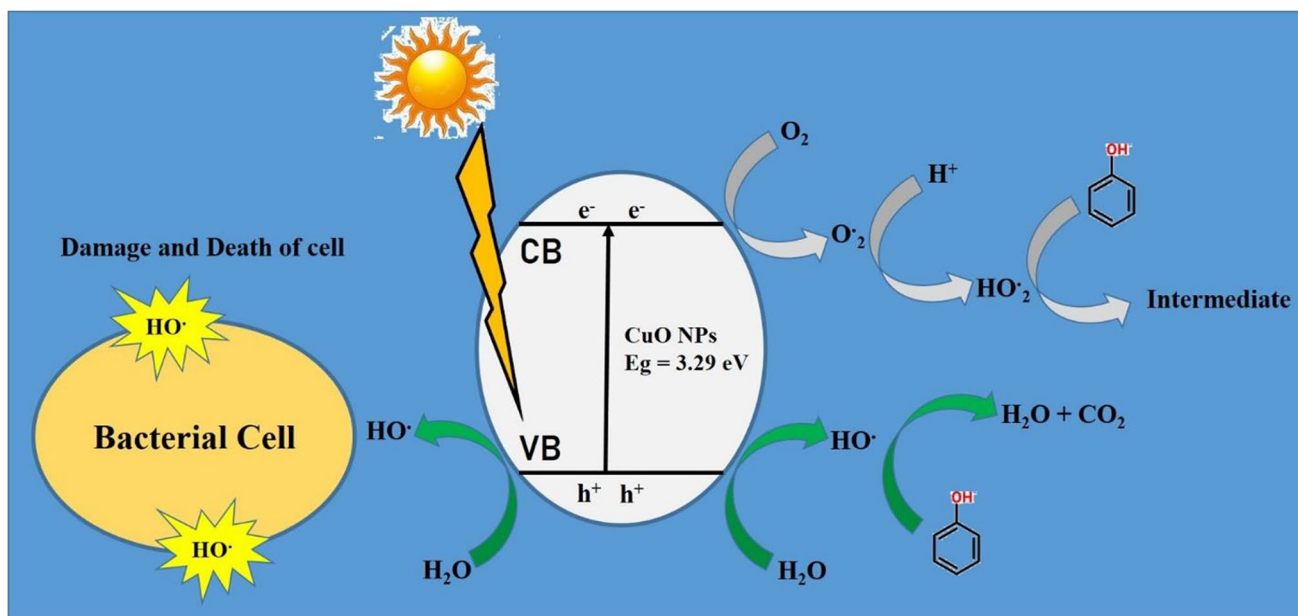


Fig. 13 A possible mechanism of photocatalytic degradation and antimicrobial activity of the human urine-mediated CuO NPs

Fig. 14 Bactericidal effect of human urine-mediated CuO NPs against gram-positive and gram-negative bacterial strain, **a** *Staphylococcus aureus* (NCIM2178), **b** *Bacillus subtilis* (NCIM2063), **c** *E. coli* (NCIM2065), **d** *P. mirabilis* (NCIM2388)

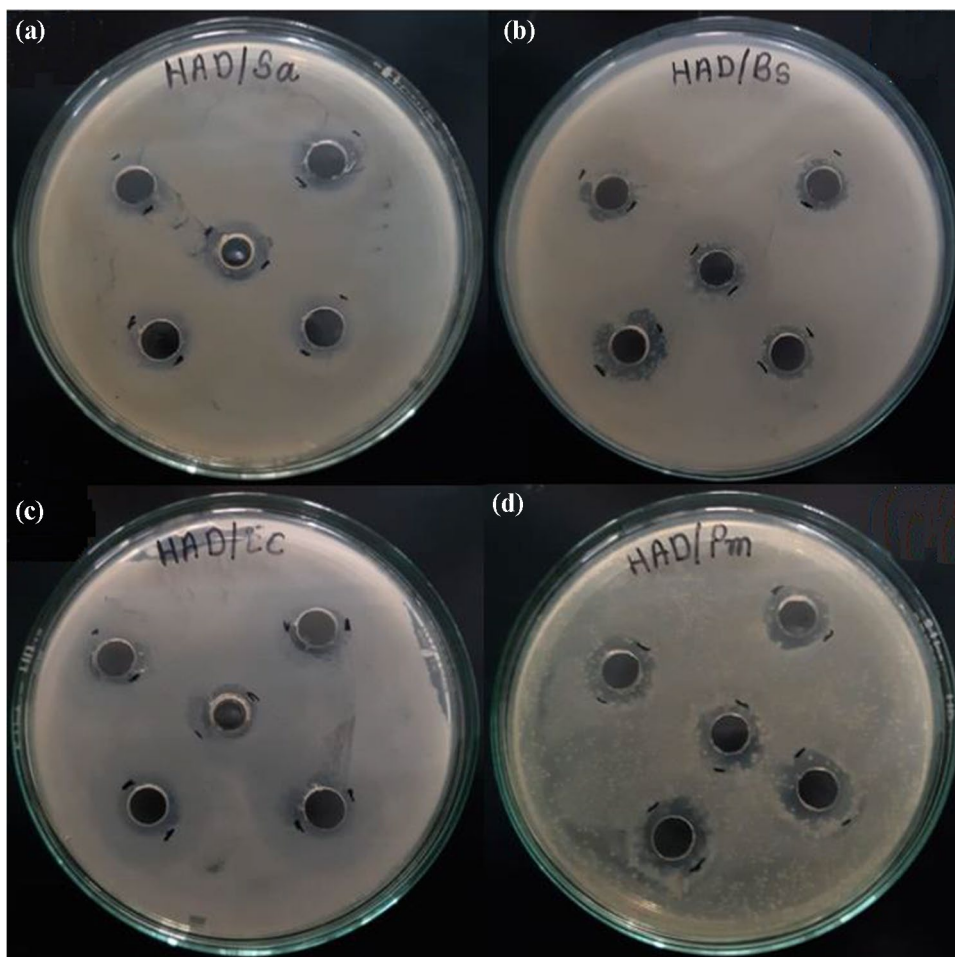
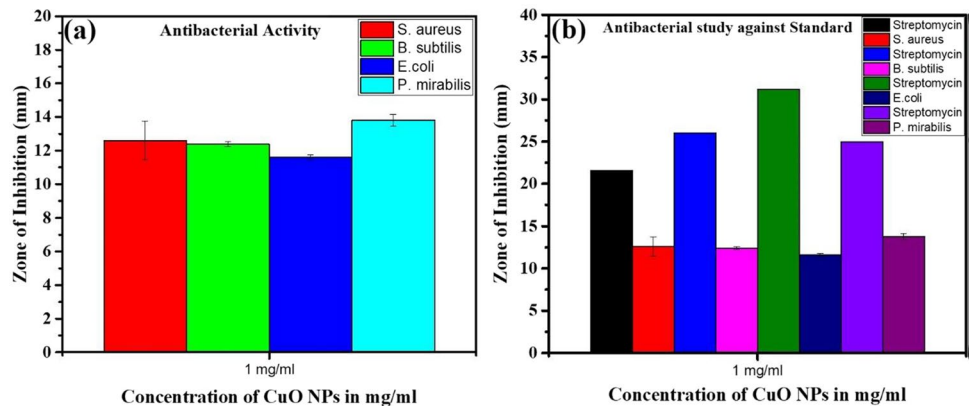
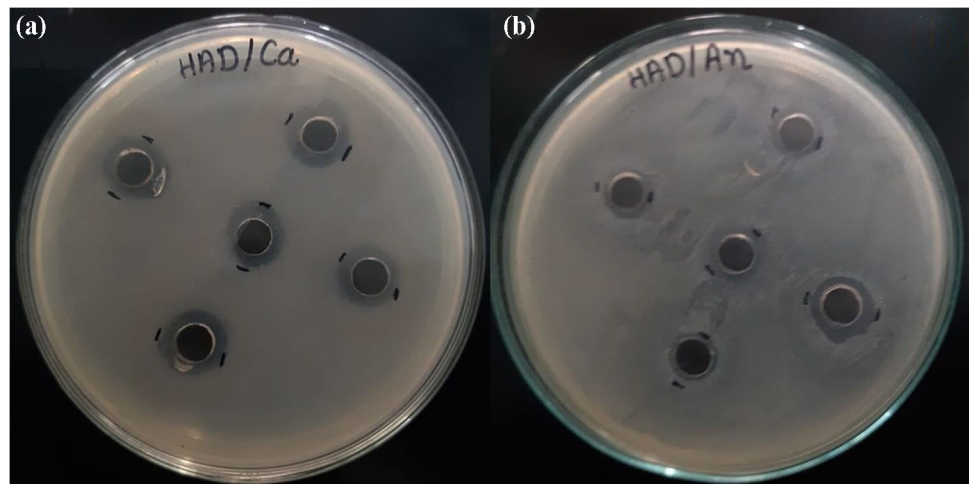


Table 1 Antibacterial activity of human urine-mediated synthesized CuO NPs

Entry	Bacterial strain	Zone of inhibition (mm)		MIC ($\mu\text{g/mL}$)	
		CuO NPs	Streptomycin	CuO NPs	Streptomycin
1	<i>S. aureus</i> (NCIM2178)	12.6 \pm 1.15	21.6	500	3.9
2	<i>B. subtilis</i> (NCIM2063)	12.4 \pm 0.15	26	500	3.9
3	<i>E. coli</i> (NCIM2065)	11.6 \pm 0.15	31.2	500	3.9
4	<i>P. mirabilis</i> (NCIM2388)	13.8 \pm 0.35	25	250	1.95

Fig. 15 Antibacterial activity; **a** zone of inhibition of synthesized CuO NPs against different bacterial strains with an error bar, **b** comparison of the zone of inhibition of synthesized CuO NPs with standard antibiotics streptomycin**Fig. 16.** Antifungal activity of synthesized CuO NPs against different fungal strains **a** *Candida albicans* (NCIM 3100) **b** *Aspergillus niger* (ATCC504)**Table 2** Antifungal performance of human urine-mediated synthesized CuO NPs

Entry	Fungal strain	Zone of inhibition (mm)		MIC ($\mu\text{g/mL}$)	
		CuO NPs	Streptomycin	CuO NPs	Streptomycin
1	<i>C. albicans</i> (NCIM 3100)	14 \pm 0.25	28	125	1.9
2	<i>A. niger</i> (ATCC504)	11.8 \pm 0.35	30	125	1.9

4 Conclusion

This work describes a unique method for synthesizing CuO NPs from human urine. The XRD pattern analysis was used to examine the synthesis and purity of CuO NPs;

the grain size was determined using Scherrer's equation and found to be 6.77 nm. BET technique was used to investigate surface attributes such as surface area, pore size, and volume distribution, obtaining 3.05 m²/g, 92.64 cm³/g, and 0.062 cm³/g, respectively. SEM, TEM, and

Fig. 17 Antifungal activity; **a** zone of inhibition of synthesized CuO NPs against different fungal strains with an error bar, **b** comparison of the zone of inhibition of synthesized CuO NPs with standard antibiotics fluconazole

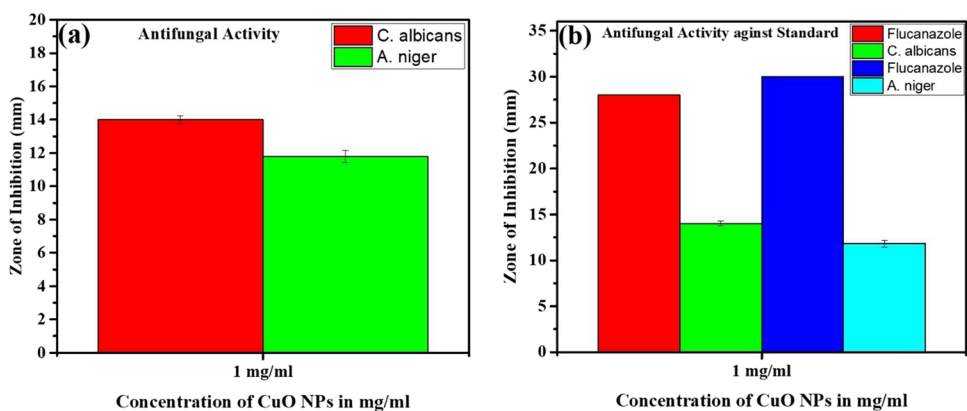


Table 3 Comparative antimicrobial study of greenly synthesized CuO NPs with previous reports

Biological entity	Size (nm)	Shape	Tested microbes (zone of inhibition in mm)	Ref.
<i>Allium sativum</i>	20–40	Spherical	<i>E. coli</i> (11.65±0.67), <i>S. aureus</i> (11.30±0.58), <i>B. subtilis</i> (10.90±0.62), <i>S. pyogenes</i> (10.65±0.60), <i>P. aeruginos</i> (10.90±0.64), <i>K. pneumoniae</i> (10.65±0.63), <i>C. albicans</i> (10.05±0.63), <i>A. flavus</i> (9.30±0.58), <i>A. fumigates</i> (9.95±0.65), and <i>A. niger</i> (9.96±0.61)	[58]
<i>Plectranthus amboinicus</i> (leaf extract)	20–35	Spherical	<i>E. coli</i> (13.65±0.88), <i>K. pneumoniae</i> (13.40±0.86), <i>P. aeruginosa</i> (13.05±0.84), <i>S. aureus</i> (13.25±0.85), <i>S. pyogenes</i> (12.55±0.80), <i>B. subtilis</i> (12.80±0.82), <i>C. albicans</i> (12.25±0.78), <i>C. tropicalis</i> (12.00±0.77), <i>A. niger</i> (11.60±0.74), and <i>A. flavus</i> (11.15±0.71)	[68]
Human urine	6.78	Pseudo-spherical	<i>S. aureus</i> (12.6±1.15), <i>B. subtilis</i> (12.4±0.15), <i>E. coli</i> (11.6±0.15), <i>P. mirabilis</i> (13.8±0.35), <i>C. albicans</i> (14±0.25), and <i>A. niger</i> (11.8±0.35)	Present work

EDS techniques confirmed the pseudo-spherical morphology and elemental composition. Finally, fully characterized CuO NPs were applied for the remediation of phenol in aqueous media. The result was compared with the previous reports and was found to be excellent. The biological activities also scan for the synthesized CuO NPs against gram-positive and gram-negative bacterial strains, and the zone of inhibition suggests excellent antibacterial properties compared with the previous report. Similarly, antifungal activity was found to be outstanding. So, considering the result, human urine-mediated synthesized CuO NPs are the best choice as photocatalysts and antimicrobial agents.

Data availability Data will be made available on request.

Author contribution Harshal Dabhane and Dhanraj Bahiram: data curation, writing—original draft. Manohar Zate: data curation, writing—original draft. Sagar Kute: data curation. Kun-Yi Andrew Lin and Abbas Rahdar: data curation, visualization, investigation. Suresh Ghotekar: data curation, visualization, investigation, writing—original draft. Balasubramani Ravindran and Deepali Sali: writing—review and editing. Chetan Ingale and Bhushan Khairnar: data curation, writing—original draft. Ghanshyam Jadhav and Vijay Medhane: data curation, writing—original draft.

Funding Not applicable.

Declarations

Ethical approval Not applicable.

Competing interests The authors declare no competing interests.

References

- Hansen SF, Arvidsson R, Nielsen MB, Hansen OFH, Clausen LPW, Baun A, Boldrin A (2022) Nanotechnology meets circular economy. *Nat Nanotechnol* 17:682–685. <https://doi.org/10.1038/s41565-022-01157-6>
- Chee P, Toh W, Yew P, Peng S, Kai D (2022) Introduction of nanotechnology and sustainability. In: Li Z, Zheng J, Ye E (eds) *Sustainable Nanotechnology*. Royal Society of Chemistry, pp 1–32. <https://doi.org/10.1039/9781839165771-00001>
- Singh A, Amiji MM (2022) Application of nanotechnology in medical diagnosis and imaging. *Curr Opin Biotechnol* 74:241–246. <https://doi.org/10.1016/j.copbio.2021.12.011>
- Ekrani E, Pouresmaieli M, Sadat Hashemiyoone E, Noorbakhsh N, Mahmoudifard M (2022) Nanotechnology: a sustainable solution for heavy metals remediation. *Environ Nanotechnol Monit Manag* 18:100718. <https://doi.org/10.1016/j.enmm.2022.100718>

5. Ghotekar S (2019) A review on plant extract mediated biogenic synthesis of CdO nanoparticles and their recent applications. *Asian J Green Chem* 3:187–200. <https://doi.org/10.22034/ajgc.2018.140313.1084>
6. Korde P, Ghotekar S, Pagar T, Pansambal S, Oza R, Mane D (2020) Plant extract assisted eco-benevolent synthesis of selenium nanoparticles—a review on plant parts involved, characterization and their recent applications. *J Chem Rev* 2:157–168. <https://doi.org/10.22034/jcr.2020.106601>
7. Ghotekar S, Pansambal S, Bilal M, Pingale SS, Oza R (2021) Environmentally friendly synthesis of Cr₂O₃ nanoparticles: characterization, applications and future perspective— a review. *Case Stud Chem Environ Eng* 3:100089. <https://doi.org/10.1016/j.csee.2021.100089>
8. Kashid Y, Ghotekar S, Bilal M, Pansambal S, Oza R, Varma RS, Nguyen V-H, Murthy HA, Mane D (2022) Bio-inspired sustainable synthesis of silver chloride nanoparticles and their prominent applications. *J Indian Chem Soc* 100335. <https://doi.org/10.1016/j.jics.2021.100335>
9. Ghotekar S, Pansambal S, Lin K-YA, Pore D, Oza R (2022) Recent advances in synthesis of CeVO₄ nanoparticles and their potential scaffold for photocatalytic applications. *Top Catal* 66(1-4):89–103. <https://doi.org/10.1007/s11244-022-01630-5>
10. Vijayakumar M, Surendhar G, Natrayan L, Patil PP, Ram P, Paramasivam P (2022) Evolution and recent scenario of nanotechnology in agriculture and food industries. *J Nanomater* 2022. <https://doi.org/10.1155/2022/1280411>
11. Zain M, Yasmeen H, Yadav SS, Amir S, Bilal M, Shahid A, Khurshid M (2022) Applications of nanotechnology in biological systems and medicine. In: *Nanotechnology for hematology, blood transfusion, and artificial blood*. Elsevier, pp 215–235. <https://doi.org/10.1016/B978-0-12-823971-1.00019-2>
12. Soni RA, Rizwan M, Singh S (2022) Opportunities and potential of green chemistry in nanotechnology. *Nanotechnol Environ Eng* 7(3):661–673. <https://doi.org/10.1007/s41204-022-00233-5>
13. Pansambal S, Oza R, Borgave S, Chauhan A, Bardapurkar P, Vyas S, Ghotekar S (2022) Bioengineered cerium oxide (CeO₂) nanoparticles and their diverse applications: a review. *Appl Nanosci*:1–26. <https://doi.org/10.1007/s13204-022-02574-8>
14. Gur T, Meydan I, Seckin H, Bekmezci M, Sen F (2022) Green synthesis, characterization and bioactivity of biogenic zinc oxide nanoparticles. *Environ Res* 204:111897. <https://doi.org/10.1016/j.envres.2021.111897>
15. Pansambal S, Roy A, Mohamed HEA, Oza R, Vu CM, Marzban A, Chauhan A, Ghotekar S (2022) Murthy H Recent developments on magnetically separable ferrite-based nanomaterials for removal of environmental pollutants. *J Nanomater*. <https://doi.org/10.1155/2022/8560069>
16. Tran TV, Nguyen DTC, Kumar PS, Din ATM, Jalil AA, Vo D-VN (2022) Green synthesis of ZrO₂ nanoparticles and nanocomposites for biomedical and environmental applications: a review. *Environ Chem Lett*:1–23. <https://doi.org/10.1007/s10311-021-01367-9>
17. Dabhane H, Ghotekar SK, Tambade PJ, Pansambal S, Ananda Murthy H, Oza R, Medhane V (2021) Cow urine mediated green synthesis of nanomaterial and their applications: a state-of-the-art review. *J Water Environ Nanotechnol* 6:81–91. <https://doi.org/10.22090/jwent.2021.01.008>
18. Wang J, Wang Z, Wang W, Wang Y, Hu X, Liu J, Gong X, Miao W, Ding L, Li X (2022) Synthesis, modification and application of titanium dioxide nanoparticles: a review. *Nanoscale*. <https://doi.org/10.1039/D1NR08349J>
19. Aswathi V, Meera S, Maria C, Nidhin M (2022) Green synthesis of nanoparticles from biodegradable waste extracts and their applications: a critical review. *Nanotechnol Environ Eng*:1–21. <https://doi.org/10.1007/s41204-022-00276-8>
20. Barwant M, Ugale Y, Ghotekar S, Basnet P, Nguyen V-H, Pansambal S, Ananda Murthy H, Sillanpaa M, Bilal M, Oza R (2022) Eco-friendly synthesis and characterizations of Ag/AgO/Ag₂O nanoparticles using leaf extracts of *Solanum elaeagnifolium* for antioxidant, anticancer, and DNA cleavage activities. *Chem Pap*:1–13. <https://doi.org/10.1007/s11696-022-02178-0>
21. Nguyen TP, Nguyen QV, Nguyen V-H, Le T-H, Huynh VQN, Vo D-VN, Trinh QT, Kim SY, Le QV (2019) Silk fibroin-based biomaterials for biomedical applications: a review. *Polymers* 11:1933. <https://doi.org/10.3390/polym11121933>
22. Madani M, Hosny S, Alshangiti DM, Nady N, Alkhursani SA, Alkhalidi H, Al-Gahtany SA, Ghobashy MM, Gaber GA (2022) Green synthesis of nanoparticles for varied applications: green renewable resources and energy-efficient synthetic routes. *Nanotechnol Rev* 11:731–759. <https://doi.org/10.1515/ntrev-2022-0034>
23. Marzban A, Mirzaei SZ, Karkhane M, Ghotekar SK, Danesh A (2022) Biogenesis of copper nanoparticles assisted with seaweed polysaccharide with antibacterial and antibiofilm properties against methicillin-resistant *Staphylococcus aureus*. *J Drug Deliv Sci Technol* 74:103499. <https://doi.org/10.1016/j.jddst.2022.103499>
24. Ateia M, Ersan G, Alalm MG, Boffito DC, Karanfil T (2022) Emerging investigator series: microplastics sources, fate, toxicity, detection, and interactions with micropollutants in aquatic ecosystems—a review of reviews. *Environ Sci: Process Impacts*. <https://doi.org/10.1039/D1EM00443C>
25. Sudhaik A, Raizada P, Ahamad T, Alshehri SM, Nguyen V-H, Van Le Q, Thakur S, Thakur VK, Selvasembian R, Singh P (2022) Recent advances in cellulose supported photocatalysis for pollutant mitigation: a review. *Int J Biol Macromol*. <https://doi.org/10.1016/j.ijbiomac.2022.11.241>
26. Shultana S, Khan RA (2022) Water quality assessment, reasons of river water pollution, impact on human health and remediation of polluted river water. *GSC Adv Res Rev* 10:107–115. <https://doi.org/10.30574/gscarr.2022.10.2.0053>
27. Alemu A, Lemma B, Gabbaye N, Alula MT, Desta MT (2018) Removal of chromium (VI) from aqueous solution using vesicular basalt: a potential low cost wastewater treatment system. *Heliyon* 4:e00682. <https://doi.org/10.1016/j.heliyon.2018.e00682>
28. Van Tran T, Nguyen DTC, Kumar PS, Din ATM, Qazaq AS, Vo D-VN (2022) Green synthesis of Mn₃O₄ nanoparticles using *Cosmos woodsonii* flowers extract for effective removal of malachite green dye. *Environ Res* 214:113925. <https://doi.org/10.1016/j.envres.2022.113925>
29. Del Rio DDF, Sovacool BK, Griffiths S, Bazilian M, Kim J, Foley AM, Rooney D (2022) Decarbonizing the pulp and paper industry: a critical and systematic review of sociotechnical developments and policy options. *Renew Sustain Energy Rev* 167:112706. <https://doi.org/10.1016/j.rser.2022.112706>
30. Saravanan A, Kumar PS, Jeevanantham S, Anubha M, Jayashree S (2022) Degradation of toxic agrochemicals and pharmaceutical pollutants: effective and alternative approaches toward photocatalysis. *Environ Pollut* 118844. <https://doi.org/10.1016/j.envpol.2022.118844>
31. Nayak R, Ali FA, Mishra DK, Ray D, Aswal V, Sahoo SK, Nanda B (2020) Fabrication of CuO nanoparticle: an efficient catalyst utilized for sensing and degradation of phenol. *J Mater Res Technol* 9:11045–11059. <https://doi.org/10.1016/j.jmrt.2020.07.100>
32. Abarian M, Hassanshahian M, Esbah A (2019) Degradation of phenol at high concentrations using immobilization of *Pseudomonas putida* P53 into sawdust entrapped in sodium-alginate beads. *Water Sci Technol* 79:1387–1396. <https://doi.org/10.2166/wst.2019.134>
33. Cabaja J, Agnieszka J, Karol M, Agnieszka Ś, Jadwiga S (2016) Optical biosensor for permanent monitoring of phenol derivatives


- in water solutions. *Chem Eng Trans* 47. <https://doi.org/10.3303/CET1647003>
34. Rao S, As S, Jayaprakash GK, Swamy MM, Kumar D (2022) Plant seed extract assisted, eco-synthesized C-ZnO nanoparticles: characterization, chromium (VI) ion adsorption and kinetic studies. *Luminescence*. <https://doi.org/10.1002/bio.4213>
35. Baishnisha A, Divakaran K, Balakumar V, Perumal KN, Meenakshi C, Kannan RS (2021) Synthesis of highly efficient g-CN@CuO nanocomposite for photocatalytic degradation of phenol under visible light. *J Alloys Compd* 886:161167. <https://doi.org/10.1016/j.jallcom.2021.161167>
36. Scott T, Zhao H, Deng W, Feng X, Li Y (2019) Photocatalytic degradation of phenol in water under simulated sunlight by an ultrathin MgO coated Ag/TiO₂ nanocomposite. *Chemosphere* 216:1–8. <https://doi.org/10.1016/j.chemosphere.2018.10.083>
37. Ling H, Kim K, Liu Z, Shi J, Zhu X, Huang J (2015) Photocatalytic degradation of phenol in water on as-prepared and surface modified TiO₂ nanoparticles. *Catal Today* 258:96–102. <https://doi.org/10.1016/j.cattod.2015.03.048>
38. Al-Hamdi AM, Sillanpää M, Bora T, Dutta J (2016) Efficient photocatalytic degradation of phenol in aqueous solution by SnO₂:Sb nanoparticles. *Appl Surf Sci* 370:229–236. <https://doi.org/10.1016/j.apsusc.2016.02.123>
39. Zhang Y, Zhao G, Xuan Y, Gan L, Pan M (2021) Enhanced photocatalytic performance for phenol degradation using ZnO modified with nano-biochar derived from cellulose nanocrystals. *Cellulose* 28:991–1009. <https://doi.org/10.1007/s10570-020-03581-0>
40. Cuong HN, Pansambal S, Ghotekar S, Oza R, Hai NTT, Viet NM, Nguyen V-H (2022) New frontiers in the plant extract mediated biosynthesis of copper oxide (CuO) nanoparticles and their potential applications: a review. *Environ Res* 203:111858. <https://doi.org/10.1016/j.envres.2021.111858>
41. Chakraborty N, Banerjee J, Chakraborty P, Banerjee A, Chanda S, Ray K, Acharya K, Sarkar J (2022) Green synthesis of copper/copper oxide nanoparticles and their applications: a review. *Green Chem Lett Rev* 15:187–215. <https://doi.org/10.1080/17518253.2022.2025916>
42. Gawande MB, Goswami A, Felpin F-X, Asefa T, Huang X, Silva R, Zou X, Zboril R, Varma RS (2016) Cu and Cu-based nanoparticles: synthesis and applications in catalysis. *Chem Rev* 116:3722–3811. <https://doi.org/10.1021/acs.chemrev.5b00482>
43. Pansambal S, Deshmukh K, Savale A, Ghotekar S, Pardeshi O, Jain G, Aher Y, Pore D (2017) Phytosynthesis and biological activities of fluorescent CuO nanoparticles using *Acanthospermum hispidum* L. extract. *J Nanostructures* 7:165–174. <https://doi.org/10.22052/JNS.2017.03.001>
44. Pagar K, Ghotekar S, Pagar T, Nikam A, Pansambal S, Oza R, Sanap D, Dabhane H (2020) Antifungal activity of biosynthesized CuO nanoparticles using leaves extract of *Moringa oleifera* and their structural characterizations. *Asian J Nanosci Mater* 3:15–23. <https://doi.org/10.26655/AJNANOMAT.2020.1.2>
45. Nagore P, Ghotekar S, Mane K, Ghoti A, Bilal M, Roy A (2021) Structural properties and antimicrobial activities of *Polyalthia longifolia* leaf extract-mediated CuO nanoparticles. *BioNanoScience* 11:579–589. <https://doi.org/10.1007/s12668-021-00851-4>
46. Dulta K, Koşarsoy Ağçeli G, Chauhan P, Jasrotia R, Chauhan P, Ighalo JO (2022) Multifunctional CuO nanoparticles with enhanced photocatalytic dye degradation and antibacterial activity. *Sustain Environ Res* 32:1–15. <https://doi.org/10.1186/s42834-021-00111-w>
47. Kannan K, Radhika D, Vijayalakshmi S, Sadasivuni KK, Ojiaku A, Verma U (2022) Facile fabrication of CuO nanoparticles via microwave-assisted method: photocatalytic, antimicrobial and anticancer enhancing performance. *Int J Environ Anal Chem* 102:1095–1108. <https://doi.org/10.1080/03067319.2020.1733543>
48. Murthy HA, Zeleke TD, Tan K, Ghotekar S, Alam MW, Balachandran R, Chan K-Y, Sanaulla P, Kumar MA, Ravikumar C (2021) Enhanced multifunctionality of CuO nanoparticles synthesized using aqueous leaf extract of *Vernonia amygdalina* plant. *Results Chem* 3:100141. <https://doi.org/10.1016/j.rechem.2021.100141>
49. Sibhatu AK, Weldegebräel GK, Sagadevan S, Tran NN, Hessel V (2022) Photocatalytic activity of CuO nanoparticles for organic and inorganic pollutants removal in wastewater remediation. *Chemosphere* 134623. <https://doi.org/10.1016/j.chemosphere.2022.134623>
50. George A, Raj DMA, Venci X, Raj AD, Irudayaraj AA, Josephine R, Sundaram SJ, Al-Mohaimeed AM, Al Farraj DA, Chen T-W (2022) Photocatalytic effect of CuO nanoparticles flower-like 3D nanostructures under visible light irradiation with the degradation of methylene blue (MB) dye for environmental application. *Environ Res* 203:111880. <https://doi.org/10.1016/j.envres.2021.111880>
51. Raizada P, Sudhaik A, Patial S, Hasija V, Khan AAP, Singh P, Gautam S, Kaur M, Nguyen V-H (2020) Engineering nanostructures of CuO-based photocatalysts for water treatment: current progress and future challenges. *Arab J Chem* 13:8424–8457. <https://doi.org/10.1016/j.arabjc.2020.06.031>
52. Aibinu AM, Folorunso TA, Saka AA, Ogunfowora LA, Iwuozor KO, Ighalo JO (2022) Green synthesis of CuO nanocomposite from watermelon (*Citrullus lanatus*) rind for the treatment of aquaculture effluent. *Reg Stud Mar Sci* 52:102308. <https://doi.org/10.1016/j.risma.2022.102308>
53. Arunkumar B, Jothibas M, Jeyakumar SJ (2022) Blue dye degradation effect of green chemical synthesized CuO nanoparticles. *Mater Today: Proc* 66:2207–2214. <https://doi.org/10.1016/j.matpr.2022.06.038>
54. Akintelu SA, Folorunso AS, Folorunso FA, Oyebamiji AK (2020) Green synthesis of copper oxide nanoparticles for biomedical application and environmental remediation. *Heliyon* 6:e04508. <https://doi.org/10.1016/j.heliyon.2020.e04508>
55. Waris A, Din M, Ali A, Ali M, Afridi S, Baset A, Khan AU (2021) A comprehensive review of green synthesis of copper oxide nanoparticles and their diverse biomedical applications. *Inorg Chem Comm* 123:108369. <https://doi.org/10.1016/j.inoche.2020.108369>
56. Chauhan A, Kumari S, Verma R, Dutta V, Ghotekar S, Kaur M, Kulshrestha S, Singh K, Lin K-YA, Kumar R (2022) Fabrication of copper oxide nanoparticles via microwave and green approaches and their antimicrobial potential. *Chem Pap*:1–16. <https://doi.org/10.1007/s11696-022-02407-6>
57. Gopinath V, Priyadarshini S, Al-Maleki A, Alagiri M, Yahya R, Saravanan S, Vadivelu J (2016) In vitro toxicity, apoptosis and antimicrobial effects of phyto-mediated copper oxide nanoparticles. *RSC Adv* 6:110986–110995. <https://doi.org/10.1039/C6RA13871C>
58. Velsankar K, Rm AK, Preethi R, Muthulakshmi V, Sudhahar S (2020) Green synthesis of CuO nanoparticles via *Allium sativum* extract and its characterizations on antimicrobial, antioxidant, antilarvicidal activities. *J Environ Chem Eng* 8:104123. <https://doi.org/10.1016/j.jece.2020.104123>
59. Zedan AF, Mohamed AT, El-Shall MS, AlQaradawi SY, AlJaber AS (2018) Tailoring the reducibility and catalytic activity of CuO nanoparticles for low temperature CO oxidation. *RSC Adv* 8:19499–19511. <https://doi.org/10.1039/C8RA03623C>
60. Murthy H, Desalegn T, Kassa M, Abebe B, Assefa T (2020) Synthesis of green copper nanoparticles using medicinal plant *hagenia abyssinica* (Brace) JF. Gmel. leaf extract: Antimicrobial properties. *J Nanomater* 2020. <https://doi.org/10.1155/2020/3924081>
61. George A, Raj DMA, Raj AD, Irudayaraj AA, Arumugam J, Prabu HJ, Sundaram SJ, Al-Dhabi NA, Arasu MV, Maaza M (2020) Temperature effect on CuO nanoparticles: antimicrobial activity

- towards bacterial strains. *Surf Interfaces* 21:100761. <https://doi.org/10.1016/j.surf.2020.100761>
62. Sarigul N, Korkmaz F, Kurultak İ (2019) A new artificial urine protocol to better imitate human urine. *Sci Rep* 9:1–11. <https://doi.org/10.1038/s41598-019-56693-4>
 63. Shammout M, Awwad A (2021) A novel route for the synthesis of copper oxide nanoparticles using Bougainvillea plant flowers extract and antifungal activity evaluation. *Chem Int* 7:71–78. <https://doi.org/10.5281/zenodo.4042902>
 64. Vanathi P, Rajiv P, Sivaraj R (2016) Synthesis and characterization of Eichhornia-mediated copper oxide nanoparticles and assessing their antifungal activity against plant pathogens. *Bull Mater Sci* 39:1165–1170. <https://doi.org/10.1007/s12034-016-1276-x>
 65. Ahmad H, Venugopal K, Bhat A, Kavitha K, Ramanan A, Rajagopal K, Srinivasan R, Manikandan E (2020) Enhanced biosynthesis synthesis of copper oxide nanoparticles (CuO-NPs) for their antifungal activity toxicity against major phyto-pathogens of apple orchards. *Pharm Res* 37:1–12. <https://doi.org/10.1007/s11095-020-02966-x>
 66. Asghar MA, Asghar MA (2020) Green synthesized and characterized copper nanoparticles using various new plants extracts aggravate microbial cell membrane damage after interaction with lipopolysaccharide. *Int J Biol Macromol* 160:1168–1176. <https://doi.org/10.1016/j.ijbiomac.2020.05.198>
 67. Meghana S, Kabra P, Chakraborty S, Padmavathy N (2015) Understanding the pathway of antibacterial activity of copper oxide nanoparticles. *RSC Adv* 5:12293–12299. <https://doi.org/10.1039/C4RA12163E>
 68. Velsankar K, Vinothini V, Sudahar S, Kumar MK, Mohandoss S (2020) Green Synthesis of CuO nanoparticles via Plecranthus amboinicus leaves extract with its characterization on structural, morphological, and biological properties. *Appl Nanosci* 10:3953–3971. <https://doi.org/10.1007/s13204-020-01504-w>

Publisher's note Springer Nature remains neutral with regard to jurisdictional claims in published maps and institutional affiliations.

Springer Nature or its licensor (e.g. a society or other partner) holds exclusive rights to this article under a publishing agreement with the author(s) or other rightsholder(s); author self-archiving of the accepted manuscript version of this article is solely governed by the terms of such publishing agreement and applicable law.

Authors and Affiliations

Harshal Dabhane¹ · Suresh Ghotekar²  · Manohar Zate³ · Kun-Yi Andrew Lin⁴ · Abbas Rahdar⁵ · Balasubramani Ravindran^{6,7} · Dhanraj Bahiram¹ · Chetan Ingale⁸ · Bhushan Khairnar⁹ · Deepali Sali¹⁰ · Sagar Kute¹¹ · Ghanshyam Jadhav¹² · Vijay Medhane^{12,13}

¹ Department of Chemistry, G.M.D. Arts, B.W. Commerce and Science College, Savitribai Phule Pune University, Sinnar, Maharashtra 422 103, India

² Department of Chemistry, Smt. Devkiba Mohansinhji Chauhan College of Commerce & Science (University of Mumbai), Silvassa, Dadra and Nagar Haveli (UT) 396 230, India

³ Department of Physics, S.V.K.T. Arts, Commerce and Science College, Savitribai Phule Pune University, Nashik, Maharashtra 422401, India

⁴ Department of Environmental Engineering & Innovation and Development Center of Sustainable Agriculture, National Chung Hsing University, 250 Kuo-Kuang Road, Taichung, Taiwan

⁵ Department of Physics, Faculty of Science, University of Zabol, Zabol P.O. Box. 35856-98613, Iran

⁶ Department of Environmental Energy and Engineering, Kyonggi University, Gyeonggi-do, Suwon-si 16227, South Korea

⁷ Department of Medical Biotechnology and Integrative Physiology, Institute of Biotechnology, Saveetha School of Engineering, Saveetha Institute of Medical and Technical Sciences, Thandalam, Chennai, Tamil Nadu 602 105, India

⁸ Department of Chemistry, R.B. Narayanrao Borawake College, Savitribai Phule Pune University, Shrirampur, Maharashtra 413709, India

⁹ Department of Microbiology, S.V.K.T. Arts, Commerce and Science College, Savitribai Phule Pune University, Nashik, Maharashtra 422401, India

¹⁰ Department of Chemistry, Loknete Vyankatrao Hiray Arts, Science and Commerce College, Nashik, India

¹¹ Department of Physics, G.M.D. Arts, B.W. Commerce and Science College, Savitribai Phule Pune University, Sinnar, Maharashtra 422 103, India

¹² Department of Chemistry, K.R.T. Arts, B.H. Commerce, and A.M. Science College, Savitribai Phule Pune University, Nashik, Maharashtra 422002, India

¹³ Department of Chemistry, Karmaveer Abasaheb alias N.M. Sonawane Arts, Commerce & Science College, Savitribai Phule Pune University, Satana, Maharashtra 423 301, India